JB
Journals.ASM.org

Flavobacterium johnsoniae RemA Is a Mobile Cell Surface Lectin Involved in Gliding

Abhishek Shrivastava,[a] Ryan G. Rhodes,[a,b] Soumya Pochiraju,[a] Daisuke Nakane,[c] and Mark J. McBride[a]

Department of Biological Sciences, University of Wisconsin–Milwaukee, Milwaukee, Wisconsin, USA[a]; Department of Biology, St. Bonaventure University, St. Bonaventure, New York, USA[b]; and Department of Molecular Microbiology and Immunology, Nagasaki University, Nagasaki, Japan[c]

Cells of *Flavobacterium johnsoniae* move rapidly over surfaces by a process known as gliding motility. Gld proteins are thought to comprise the motor that propels the cell surface adhesin SprB. Cells with mutations in *sprB* are partially defective in motility and are also resistant to some bacteriophages. Transposon mutagenesis of a strain carrying a deletion spanning *sprB* identified eight mutants that were resistant to additional phages and exhibited reduced motility. Four of the mutants had transposon insertions in *remA*, which encodes a cell surface protein that has a lectin domain and appears to interact with polysaccharides. Three other genes identified in this screen (*remC*, *wza*, and *wzc*) encode proteins predicted to be involved in polysaccharide synthesis and secretion. Myc-tagged versions of RemA localized to the cell surface and were propelled rapidly along the cell at speeds of 1 to 2 μm/s. Deletion of *gldN* and *gldO*, which encode components of a bacteroidete protein secretion system, blocked the transport of RemA to the cell surface. Overexpression of RemA resulted in the formation of cell aggregates that were dispersed by the addition of galactose or rhamnose. Cells lacking RemC, Wza, and Wzc failed to aggregate. Cells of a *remC* mutant and cells of a *remA* mutant, neither of which formed aggregates in isolation, aggregated when they were mixed together, suggesting that polysaccharides secreted by one cell may interact with RemA on another cell. Fluorescently labeled lectin *Ricinus communis* agglutinin I detected polysaccharides secreted by *F. johnsoniae*. The polysaccharides bound to cells expressing RemA and were rapidly propelled on the cell surface. RemA appears to be a mobile cell surface adhesin, and secreted polysaccharides may interact with the lectin domain of RemA and enhance motility.

Cells of *Flavobacterium johnsoniae* and of many other members of the phylum *Bacteroidetes*, translocate rapidly over surfaces in a process called gliding motility (19). These cells do not have well-studied bacterial motility organelles, such as flagella or pili. Instead, they rely on a novel motility apparatus composed of proteins that are unique to the phylum *Bacteroidetes*. Nineteen proteins involved in motility have been identified (2, 3, 20, 26, 27, 31, 34). SprB is a cell surface protein that appears to be propelled rapidly by the motility machinery (26). Some of the motility proteins (GldK, GldL, GldM, GldN, SprA, SprE, and SprT) are thought to comprise a protein secretion system, the PorSS, that is needed for delivery of SprB to the cell surface and for secretion of an extracellular chitinase (33–35). The PorSS is not related to the type I to type VI protein secretion systems. Other Gld proteins are likely components of the motors that propel SprB along the cell surface.

Disruption of *sprB* results in the formation of nonspreading colonies, in contrast to the thin spreading colonies produced by wild-type cells. However, *sprB* mutant cells retain some ability to crawl on glass surfaces (26). This suggested the possibility that SprB is a semiredundant component of the motility machinery. Analysis of the genome sequence revealed many *sprB* paralogs, any of which might explain the residual motility exhibited by *sprB* mutants (24).

Disruption of *F. johnsoniae* motility genes results not only in motility defects but also in resistance to bacteriophages that infect wild-type cells. Completely nonmotile *gld* mutants are resistant to infection by all bacteriophages, whereas most mutants with partial motility defects are resistant to some but not all phages (33). *sprB* mutants display increased resistance to *F. johnsoniae* phages ϕCj1, ϕCj13, ϕCj23, and ϕCj29 but are sensitive to ϕCj28, ϕCj42, ϕCj48, and ϕCj54 (26). SprB may function as a phage receptor, and other cell surface components of the motility machinery may also interact with specific phages.

In the present study we conducted *HimarEm1* mutagenesis of an *sprB* mutant and identified eight mutants that exhibited resistance to additional bacteriophages. Cells of the mutants exhibited more severe motility defects than did the parent strain, suggesting that the disrupted genes encode proteins involved in cell movement. The genes mutated included the *sprB*-like gene *remA*, which encodes a cell surface protein with a lectin domain, and genes likely to be involved in polysaccharide synthesis or export. The results support the hypothesis that there is redundancy in the cell surface components of the motility machinery, and that multiple cell surface proteins, such as RemA and SprB, may function as mobile adhesins to allow interaction with and movement over diverse surfaces.

MATERIALS AND METHODS

Bacterial strains, bacteriophage, plasmids, and growth conditions. *F. johnsoniae* UW101, which is derived from the type strain ATCC 17061, was the wild-type strain used in the present study (4, 22, 24). The streptomycin-resistant *rpsL* mutant of UW101 (CJ1827) was used to construct strains with unmarked deletions and gene replacements (32). *F. johnsoniae* strains were grown in Casitone-yeast extract (CYE) medium at

Received 7 April 2012 Accepted 3 May 2012
Published ahead of print 11 May 2012
Address correspondence to Mark J. McBride, mcbride@uwm.edu.
Supplemental material for this article may be found at http://jb.asm.org/.

doi:10.1128/JB.00588-12

30°C, as previously described (23). To observe colony spreading, *F. johnsoniae* was grown at 25°C on PY2 medium (1) or EC medium (4) supplemented with 10 g of agar per liter. Motility medium (MM) (17) and EC medium were used to observe movement of individual cells in wet mounts. The bacteriophages active against *F. johnsoniae* that were used here were ϕCj1, ϕCj13, ϕCj23, ϕCj28, ϕCj29, ϕCj42, ϕCj48, and ϕCj54 (4, 28, 42). Sensitivity to bacteriophages was determined essentially as previously described by spotting 5 μl of phage lysates (10^9 PFU/ml) onto lawns of cells in CYE overlay agar (11). The plates were incubated for 24 h at 25°C to observe lysis. The strains and plasmids used in the present study are listed in Table 1. The plasmids used for complementation were all derived from pCP1 and have copy numbers of approximately 10 in *F. johnsoniae* (1, 13, 23). Antibiotics were used at the following concentrations when needed: ampicillin, 100 μg/ml; cefoxitin, 100 μg/ml; chloramphenicol, 30 μg/ml; erythromycin, 100 μg/ml; kanamycin, 35 μg/ml; and tetracycline, 20 μg/ml.

Isolation of phage-resistant mutants of *F. johnsoniae* CJ1584 [Δ(*sprC sprD sprB*)] by *HimarEm1* mutagenesis and identification of sites of insertion. pHimarEm1 was introduced into *F. johnsoniae* CJ1584 by conjugation from *Escherichia coli* S17-1 λ*pir* essentially as previously described (2). *HimarEm1* mutants were selected by plating cells on CYE agar containing erythromycin. Cells from 800 random erythromycin-resistant colonies were transferred to CYE agar (master plate) and to CYE agar overlaid with 4 ml of CYE top agar containing ~10^9 PFU of ϕCj42, followed by incubation for 24 h at 25°C. Colonies that grew in the presence of ϕCj42 were picked from the corresponding colonies on the master plate and streaked for isolation on CYE with erythromycin. Colonies were tested again for phage sensitivity, and those with increased resistance were selected for further analyses.

Chromosomal DNA was isolated from each of the phage-resistant mutants, and the *HimarEm1* transposons and adjacent DNA from each were cloned in *E. coli* EC100D pir^+. Sequences of *F. johnsoniae* DNA disrupted by *HimarEm1* were determined as previously described (2).

Strain construction. Unmarked deletions were made as previously described (32). To delete *remA*, a 1.8-kbp fragment spanning *fjoh_0809* and the final 72 bp of *remA* was amplified by PCR using the primers 1061 (introducing a SalI site) and 760 (introducing a PstI site). The fragment was digested with SalI and PstI and ligated into pRR51 that had been digested with the same enzymes to generate pRR76. A 2.1-kbp fragment spanning *fjoh_0807* and the first 150 bp of *remA* was amplified by PCR with primers 1059 (introducing a BamHI site) and 1060 (introducing a SalI site). The fragment was digested with BamHI and SalI and fused to the region downstream of *remA* by ligation with pRR76 that had been digested with the same enzymes to generate the deletion construct pRR78. Plasmid pRR78 was introduced into the streptomycin-resistant wild-type *F. johnsoniae* strain CJ1827 and into the *sprB* deletion mutant CJ1922 by triparental conjugation, and *remA* deletion mutants were isolated as previously described (32). Deletion of *remA* was confirmed by PCR amplification using the primers 778 and 1062, which flank *remA*, and sequencing the resulting 1.8-kbp product. All other deletion strains listed in Table 1 except for CJ2089 [*rpsL2* Δ(*gldN gldO*) *remA*::myc-tag-1] and CJ2090 [*rpsL2* Δ(*gldN gldO*)] were constructed in the same way, using the primers listed in Table S1 in the supplemental material and the plasmids listed in Table 1. CJ2089 and CJ2090 were constructed as previously described (33) by introducing pNap3 into CJ2083 or CJ1827, respectively, selecting for antibiotic-resistant colonies that had the plasmid inserted in the genome and then selecting for resistance to ϕCj1 to obtain the *gldNO* deletions. The *sprF* mutant CJ2097 was constructed by integration of pRR47, which carries an internal fragment of *sprF*, into the chromosome of CJ2083 essentially as previously described (31).

To observe RemA on the cell surface, four strains expressing RemA containing the myc tag sequence (EQKLISEEDL) at different locations were generated using a previously described allelic-exchange method (32). As an example, to generate the strain carrying *remA*::myc-tag-1 (CJ2083), the primers 1059 (introducing a BamHI site) and 1112 (introducing the *myc* tag) were used to amplify a 2.1-kbp fragment spanning *fjoh_0807* and the first 150 bp of *remA*. Similarly, the primers 761 (introducing a SalI site) and 1110 (introducing the *myc* tag) were used to amplify the 2.4-kbp fragment beginning at bp 151 of *remA*. The two PCR products were then used as templates in a crossover PCR with the primers 761 and 1059. The resulting 4.5-kbp PCR product was digested with BamHI and SalI and ligated into the pRR51 suicide vector to generate pRR92. Plasmid pRR92 was introduced into the streptomycin-resistant wild-type strain CJ1827 and the *sprB* deletion mutant CJ1922 by triparental conjugation, and allelic exchange was performed as previously described (32). Replacement of wild-type *remA* with the *remA*::myc-tag-1 allele was confirmed by PCR amplification using primers 1142 (myc-tag sequence) and 1063 (complementary to the *remA* sequence), and sequencing the resulting 0.6-kbp product. Four different *remA*::myc-tag strains were generated, with *remA*::myc-tag-1, *remA*::myc-tag-3, *remA*::myc-tag-4, and *remA*::myc-tag-5 inserted 150, 2,058, 2,286, and 2,514 bp downstream of the "A" in the start codon, respectively.

Cloning of *remA* and complementation of *remA* mutants. Attempts to clone *remA* amplified by PCR were not successful, so an alternative approach was used. The plasmids pMM332 and pMM336 that were used to sequence *remA HimarEm1* insertions served as raw material to reconstruct the intact *remA* gene. The 3′ end of *remA* was obtained as a SphI-XbaI fragment from pMM336. This fragment was ligated into pUC18 that had been digested with the same enzymes to generate pRR36. The 5′ end of *remA* and upstream sequences were obtained as a HindIII-SphI fragment from pMM332. This fragment was inserted into pRR36 that had been digested with HindIII and SphI to generate pRR37, which carries the intact *remA* gene. *remA* was transferred to pBC SK+ as a 4.9-kbp HindIII-XbaI fragment generating pRR38. This provided convenient restriction sites (KpnI and XbaI) to allow transfer of *remA* into the shuttle vector pCP23, generating pRR39. pRR39 was introduced into *remA* mutants by conjugation as previously described (11, 21), except that pRK2013 (5) was used for triparental conjugations.

Expression of recombinant RemA in *E. coli* and generation of antibodies. A 1,966-bp fragment encoding the 561-amino-acid C-terminal region of RemA was amplified using Phusion DNA polymerase (New England Biolabs, Ipswich, MA) and the primers 745 and 762. The PCR product was digested with BamHI and SalI and cloned into the pMAL-c2 expression vector (New England Biolabs) that had been digested with the same enzymes, generating pSP18. pSP18 was introduced into *E. coli* Rosetta 2 (DE3) cells (Novagen, Madison, WI), which expressed seven rare tRNAs required for the efficient expression of RemA. To isolate recombinant RemA, cells were grown to mid-log phase at 37°C in rich medium containing glucose (10 g of tryptone, 5 g of yeast extract, 5 g of NaCl, and 2 g of glucose/liter), induced by the addition of 0.3 mM IPTG (isopropyl-β-D-thiogalactopyranoside), and incubated for 8 h at 25°C. Cells were disrupted using a French press, and recombinant RemA was purified using an amylose resin column (New England Biolabs). Polyclonal antibodies against recombinant RemA were produced and affinity purified using the recombinant protein by ProteinTech Group, Inc. (Chicago, IL).

Immunodetection and localization of RemA. *F. johnsoniae* cells were grown to mid-log phase in CYE at 25°C. Whole cells were centrifuged at 4,000 × *g*, resuspended in SDS-PAGE loading buffer, and boiled for 5 min. Proteins were separated by SDS-PAGE, and Western blot analyses were performed essentially as previously described (33) using affinity-purified antisera against RemA (1:1,000 dilution) or antisera against the c-*myc* epitope (1:10,000 dilution; AbCam, Cambridge, MA). To determine the localization of RemA, cells were disrupted with a French press and fractionated into soluble and insoluble fractions as described previously by centrifugation at 352,900 × *g* for 30 min (34), and Western blotting was performed as described above.

Microscopic observations of cell movement. Wild-type and mutant cells of *F. johnsoniae* were examined for movement over glass by phase-contrast microscopy. Tunnel slides were prepared essentially as described previously (38) using Nichiban NW-5 double-sided tape (Nichiban Co.,

TABLE 1 Strains and plasmids used in this study

Strain or plasmid	Genotype and/or description[a]	Source or reference
Strains		
UW101 (ATCC 17061)	Wild type	22, 24
CJ1584	Δ(*sprC sprD sprB*)	31
CJ1595	Δ(*sprC sprD sprB*) *remA*::*HimarEm1*; (Em^r)	This study
CJ1596	Δ(*sprC sprD sprB*) *remA*::*HimarEm1*; (Em^r)	This study
CJ1597	Δ(*sprC sprD sprB*) *remA*::*HimarEm1*; (Em^r)	This study
CJ1598	Δ(*sprC sprD sprB*) *wza*::*HimarEm1*; (Em^r)	This study
CJ1600	Δ(*sprC sprD sprB*) *remC*::*HimarEm1*; (Em^r)	This study
CJ1601	Δ(*sprC sprD sprB*) *remA*::*HimarEm1*; (Em^r)	This study
CJ1602	Δ(*sprC sprD sprB*) *wzc*::*HimarEm1*; (Em^r)	This study
CJ1603	Δ(*sprC sprD sprB*) *remB*::*HimarEm1*; (Em^r)	This study
CJ1827	*rpsL2*; (Sm^r) "wild-type" strain used in the construction of deletion mutants	32
CJ1922	*rpsL2* Δ*sprB*; (Sm^r)	32
CJ1984	*rpsL2* Δ*remA*; (Sm^r)	This study
CJ1985	*rpsL2* Δ*sprB* Δ*remA*; (Sm^r)	This study
CJ1986	*rpsL2* Δ(*fjoh_0803-fjoh_0806*); (Sm^r)	This study
CJ1987	*rpsL2* Δ*sprB* Δ(*fjoh_0803-fjoh_0806*); (Sm^r)	This study
CJ2072	*rpsL2* Δ*sprB remA*::myc-tag-1; (Sm^r)	This study
CJ2073	*rpsL2 remA*::myc-tag-5; (Sm^r)	This study
CJ2077	*rpsL2 remA*::myc-tag-3; (Sm^r)	This study
CJ2083	*rpsL2 remA*::myc-tag-1; (Sm^r)	This study
CJ2089	*rpsL2* Δ(*gldN gldO*) *remA*::myc-tag-1; (Sm^r)	This study
CJ2090	*rpsL2* Δ(*gldN gldO*); (Sm^r)	This study
CJ2097	*rpsL2 remA*::myc-tag-1 *sprF*; (Sm^r Em^r)	This study
CJ2098	*rpsL2* Δ*remA* Δ(*fjoh_0803-fjoh_0806*); (Sm^r)	This study
CJ2100	*rpsL2* Δ*sprB* Δ*remA* Δ(*fjoh_0803-fjoh_0806*); (Sm^r)	This study
CJ2112	*rpsL2 remA*::myc-tag-4; (Sm^r)	This study
Plasmids		
pBC SK+	ColE1 ori; Cm^r	Stratagene
pMAL-c2	MalE fusion protein expression vector; Ap^r	New England Biolabs
pUC18	ColE1 ori; Ap^r	39
pCP23	*E. coli-F. johnsoniae* shuttle plasmid; Ap^r $(Tc)^r$	1
pCP29	*E. coli-F. johnsoniae* shuttle plasmid; Ap^r (Cf^r Em^r)	13
pLYL03	Plasmid carrying *ermF* gene; Ap^r (Em^r)	15
pHimarEm1	Plasmid carrying *HimarEm1*; Km^r (Em^r)	2
pMM332	Plasmid generated by self-ligation of XbaI fragment spanning the site of insertion of *HimarEm1* in *remA* mutant CJ1597; Km^r (Em^r)	This study
pMM336	Plasmid generated by self-ligation of XbaI fragment spanning the site of insertion of *HimarEm1* in *remA* mutant CJ1601; Km^r (Em^r)	This study
pNap3	Plasmid for construction of *gldNO* deletion strains; Ap^r (Em^r)	33
pRR36	3,274-bp SphI-XbaI fragment of pMM336 spanning the 3′ end of *remA* inserted into pUC18; Ap^r	This study
pRR37	1,592-bp HindIII-SphI fragment of pMM332 spanning the 5′ end of *remA* inserted into pRR36; Ap^r	This study
pRR38	4.9-kbp HindIII-XbaI fragment of pRR37 spanning *remA* inserted into pBC SK+; Cm^r	This study
pRR39	4.9-kbp KpnI-XbaI fragment of pRR38 spanning *remA* inserted into pCP23; Ap^r (Tc^r)	This study
pRR47	847-bp region within *sprF* amplified with the primers 946 and 953, cloned into the XbaI and SphI sites of pLYL03; used for the construction of CJ2097; Ap^r (Em^r)	This study
pRR51	*rpsL*-containing suicide vector; Ap^r (Em^r)	32
pRR76	1.8-kbp region downstream of *remA* amplified with the primers 760 and 1061, cloned into the SalI and PstI sites of pRR51; Ap^r (Em^r)	This study
pRR77	1.9-kbp region upstream of *fjoh_0806* amplified with the primers 1062 and 1063, cloned into the SalI and SphI sites of pRR51; Ap^r (Em^r)	This study
pRR78	Construct used to delete *remA*; 2.1-kbp region upstream of *remA* amplified with the primers 1059 and 1060 and cloned into the BamHI and SalI sites of pRR76; Ap^r (Em^r)	This study
pRR79	Construct to delete *fjoh_0803* to *fjoh_0806*; 1.9-kbp region downstream of *fjoh_0803* amplified with the primers 757 and 758 and cloned into the BamHI and SalI sites of pRR77; Ap^r (Em^r)	This study
pRR92	4.5-kbp fragment amplified using the primers 761 and 1059 and containing the myc-tag sequence (introduced using the primers 1110 and 1112), inserted into pRR51; used to construct *remA*::myc-tag-1 strains; Ap^r (Em^r)	This study

(Continued on following page)

TABLE 1 (Continued)

Strain or plasmid	Genotype and/or description[a]	Source or reference
pRR93	4.4-kbp fragment amplified using the primers 738 and 745 and containing the myc-tag sequence (introduced using the primers 1126 and 1128), inserted into pRR51; used to construct *remA*::myc-tag-5 strains; Ap^r (Em^r)	This study
pRR95	4.4-kbp fragment amplified using the primers 738 and 745 and containing the myc-tag sequence (introduced using the primers 1118 and 1120), inserted into pRR51; used to construct *remA*::myc-tag-3 strains; Ap^r (Em^r)	This study
pRR96	4.4-kbp fragment amplified using the primers 738 and 745 and containing the myc-tag sequence (introduced using the primers 1122 and 1124), inserted into pRR51; used to construct *remA*::myc-tag-4 strains; Ap^r (Em^r)	This study
pSN60	pCP29 carrying *sprB*; Ap^r (Cf^r Em^r)	26
pSP18	1.96-kbp fragment encoding the 561-amino-acid C-terminal fragment of the RemA protein, inserted between the BamHI and SalI sites of pMAL-c2; Ap^r	This study
pTB79	pCP23 carrying *gldN*; Ap^r (Tc^r)	2

[a] Ampicillin resistance, Ap^r; cefoxitin resistance, Cf^r; chloramphenicol resistance, Cm^r; erythromycin resistance, Em^r; kanamycin resistance, Km^r; streptomycin resistance, Sm^r; tetracycline resistance, Tc^r. Unless indicated otherwise, the antibiotic resistance phenotypes are those expressed in *E. coli*. The antibiotic resistance phenotypes given in parentheses are those expressed in *F. johnsoniae* but not in *E. coli*.

Tokyo, Japan) to hold a glass coverslip over a glass slide. Cells in MM were introduced into the tunnel slide, incubated for 5 min, and observed for motility using an Olympus BH-2 phase-contrast microscope with a heated stage set at 25°C. Images were recorded using a Photometrics CoolSNAP$_{cf}^2$ camera and analyzed using MetaMorph software (Molecular Devices, Downingtown, PA).

Binding and movement of protein G-coated polystyrene spheres. Movement of surface-localized myc-tagged RemA was detected essentially as previously described for movement of SprB (26). Cells were grown overnight at 25°C in MM without shaking. Antibodies against myc tag peptide (1 μl of a 1:10 dilution of a 1-mg/ml stock), 0.5-μm-diameter protein G-coated polystyrene spheres (1 μl of a 0.1% stock preparation; Spherotech, Inc., Libertyville, IL), and bovine serum albumin (1 μl of a 1% solution) were added to 7 μl of cells (approximately 5×10^8 cells per ml) in MM. The presence of protein G on the spheres and the addition of bovine serum albumin eliminated nonspecific binding of spheres to cells, as previously reported (26, 31–34). The cells were introduced into a tunnel slide and examined by phase-contrast microscopy at 25°C. Samples were examined 2 min after introduction into a tunnel slide, and images were captured for 30 s.

Detection of RemA by immunofluorescence microscopy. Cells were grown overnight at 25°C in MM without shaking. Antibodies specific for the myc tag peptide (1 μl of a 1:10 dilution of a 1-mg/ml stock), F(ab′) fragment of goat anti-rabbit IgG conjugated to Alexa 488 (1.5 μl of a 1:10 dilution of a 2-mg/ml stock; Invitrogen, Carlsbad, CA), and bovine serum albumin (1 μl of a 1% solution) were added to 7 μl of cells (approximately 5×10^8 cells per ml) in MM. The cells were spotted on a glass slide, covered with a glass coverslip, and observed using a Nikon Eclipse 50i microscope. To observe the cells and the rapidly moving fluorescent signals at the same time, a combination of low-light phase-contrast microscopy and fluorescence microscopy was used. Images were recorded using a Photometrics CoolSNAP$_{ES}$ camera and were deconvoluted and analyzed using MetaMorph software.

Detection of cell surface polysaccharides by immunofluorescence microscopy using the galactose/*N*-acetylgalactosamine-binding lectin RCA$_{120}$. Cultures (10 ml) were grown overnight in test tubes (150 mm by 25 mm) at 23°C in EC media with appropriate antibiotics on a platform shaker set at 120 rpm. The cultures in test tubes were mixed gently, and 7 μl of appropriate culture was mixed with rhodamine-labeled RCA$_{120}$ (4 μl of a 1:10 dilution of a 2-mg/ml stock; Vector Laboratories, Burlingame, CA). Then, 7 μl of the sample was introduced into tunnel slides. Samples were observed with epifluorescence illumination and with epifluorescence in combination with phase contrast, using a Nikon Eclipse 50i microscope, and recorded using a Photometrics CoolSNAP$_{ES}$ camera. Images were deconvoluted and analyzed using MetaMorph software.

Cell agglutination. Cultures (10 ml) were grown overnight in test tubes (150 mm by 25 mm) at 23°C in EC medium with appropriate antibiotics on a platform shaker set at 120 rpm. Strains displaying agglutination had the majority of the biomass at the bottom of the test tubes, while strains not exhibiting agglutination were turbid throughout. The cultures in test tubes were mixed gently, and 7-μl samples were introduced into tunnel slides and observed by phase-contrast microscopy using a Photometrics Coolsnap$_{cf}^2$ camera. To measure the optical density (OD), cultures were grown as described above, samples were collected from the top of the tubes, and the OD was measured at 600 nm (OD_{600}). After initial measurements were taken, D-galactose was added to a concentration of 5 mM, followed by incubation for 5 min to disperse aggregates, and the optical density was determined again as a measure of total cell mass per tube. Strains that failed to agglutinate were also mixed with other nonagglutinating strains to determine whether the combinations would agglutinate. Cells were grown as described above and 5 ml each of the appropriate cultures were mixed in test tubes (150 mm by 25 mm). The tubes were incubated at 23°C with shaking for an additional 60 min, and cell aggregation was observed as described above.

The effect of various sugars on agglutination was determined. A 150-ml culture of wild-type *F. johnsoniae* CJ1827 carrying pRR39 was grown overnight at 23°C in EC medium with tetracycline on a tabletop shaker at 120 rpm in an Erlenmeyer flask. Then, 9.5 ml of culture was transferred to test tubes containing 0.5 ml of appropriate 100 mM sugar stock solutions or 0.5 ml of water. The tubes were incubated with shaking (120 rpm on a platform shaker) at 23°C for 60 min, and cell aggregation was observed as described above.

RESULTS

Isolation of bacteriophage-resistant mutants and identification of sites of the mutations. In an attempt to identify novel motility genes, *HimarEm1* mutagenesis was conducted on *F. johnsoniae* mutant CJ1584, which has a deletion spanning *sprC*, *sprD*, and *sprB* (31). Cells of CJ1584 form nonspreading colonies on agar that are indistinguishable from those of completely nonmotile *gld* mutants, but individual cells exhibit some movement on glass surfaces (31). Cells of nonmotile *gld* mutants are resistant to all bacteriophages that infect the wild type (2, 33). In contrast, cells of CJ1584 display increased resistance to some bacteriophages (ϕCj1, ϕCj13, ϕCj23, and ϕCj29), but they remain sensitive to

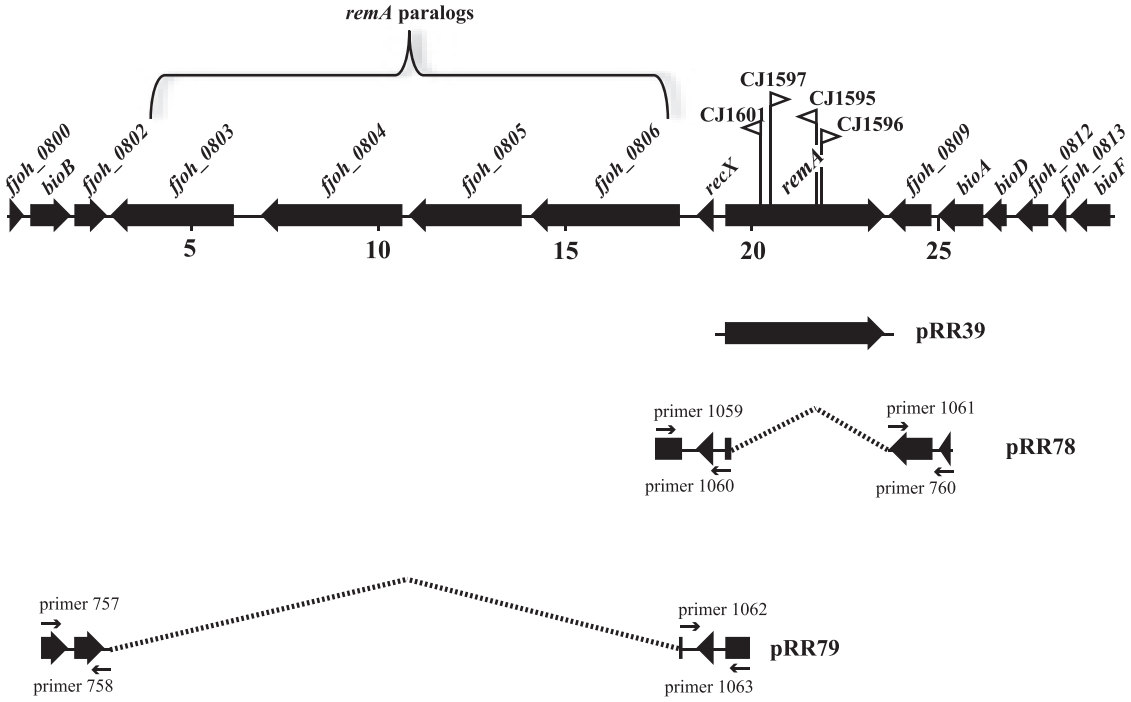

FIG 1 Map of the *remA* region. Numbers below the map refer to kilobase pairs of sequence. The sites of *HimarEm1* insertions in *remA* are indicated by triangles, with orientations indicated by the direction in which the triangle is pointing. Triangles pointing to the right in this diagram (CJ1597 for example) have IR2 on the right side and the kanamycin resistance gene of the transposon reading toward the right. The regions of DNA carried by plasmids used in the present study are indicated beneath the map.

others (ϕCj28, ϕCj42, ϕCj48, and ϕCj54) (see Fig. S1 in the supplemental material). A total of 800 randomly chosen erythromycin-resistant colonies containing *HimarEm1* insertions were screened for resistance to ϕCj42, and eight mutants with partial or complete resistance were obtained. In addition to resistance to ϕCj42, the mutants exhibited increased resistance to other phages to which CJ1584 is susceptible (see Fig. S1 in the supplemental material). Microscopic examination revealed that each mutant also had a more severe motility defect than did the parent strain (see Movie S1 in the supplemental material, and data not shown).

The sites of the transposon insertions were determined by cloning *HimarEm1* and adjacent DNA and sequencing across the junction. Four of the mutants had insertions in *fjoh_0808*, which we named *remA* (for redundant motility gene A) (Fig. 1). *remA* encodes a predicted 152-kDa protein (after removal of its signal peptide) that exhibits limited similarity to the much larger (669-kDa) cell surface motility protein SprB (26). Similarity to SprB was confined to 5 regions of RemA (amino acids 158 to 225, 453 to 494, 580 to 642, 976 to 1022, and 1282 to 1370) and ranged from 26 to 43% identity. BLASTP analysis also revealed similarity to two conserved domains of known function. The C-terminal 80 amino acids exhibited similarity to a Por secretion system C-terminal sorting domain (TIGR04183; E-value 6.93e-05), suggesting that, like SprB, RemA may be secreted across the outer membrane by the *F. johnsoniae* PorSS. In addition, the region between amino acids 725 and 800 exhibited similarity to SUEL-related galactose/rhamnose-binding lectins (pfam02140; E-value 2.44e-17), suggesting that RemA may interact with sugars. The remaining four mutants had insertions in *fjoh_1657* (*remB*), *fjoh_0216* (*remC*), *fjoh_0361* (*wza*), and *fjoh_0360* (*wzc*). RemB is predicted to be an outer membrane protein of unknown function, RemC is a predicted glycosyltransferase, and Wza and Wzc are predicted components of a polysaccharide synthesis and secretion system. Secreted or cell surface polysaccharides have previously been implicated in gliding of *F. johnsoniae* and of other bacteria (7, 8, 16, 18, 41, 43).

SprB, SprC, and SprD are each required for efficient motility on agar and for the formation of spreading colonies (26, 31). SprB is a mobile cell surface adhesin, and SprC and SprD are thought to support SprB function. Disruption of *sprB* results in increased resistance to ϕCj1, ϕCj13, ϕCj23, and ϕCj29, whereas the disruption of *sprC* and *sprD* does not result in resistance to phages that have been tested (31). CJ1985 (Δ*sprB* Δ*remA*) and CJ1984 (Δ*remA*) were constructed to simplify determination of the roles of *remA* and *sprB* in phage resistance and motility. Cells of CJ1985 (Δ*sprB* Δ*remA*) exhibited the same phage resistance phenotypes as those of CJ1601 [Δ(*sprC sprD sprB*) *remA*::*HimarEm1*] (Fig. 2; see Fig. S1 in the supplemental material). Cells of CJ1984 (Δ*remA*) exhibited increased resistance to ϕCj42, ϕCj48, and ϕCj54, and the introduction of *remA* on pRR39 restored sensitivity to these phages (Fig. 2).

Deletion of *remA* in an *sprB* mutant results in decreased motility. Cells of CJ1984 (Δ*remA*), CJ1922 (Δ*sprB*), and CJ1985 (Δ*sprB* Δ*remA*) were examined for motility (see Movies S2 and S3 in the supplemental material). Cells of CJ1984 (Δ*remA*) were indistinguishable from wild-type cells, whereas cells of CJ1922 (Δ*sprB*) exhibited a partial motility defect similar to that of CJ1584 [Δ(*sprC sprD sprB*)], as previously reported (26, 31, 32). CJ1922 formed nonspreading colonies on agar, but individual cells retained some ability to move on glass surfaces. Cells of CJ1985

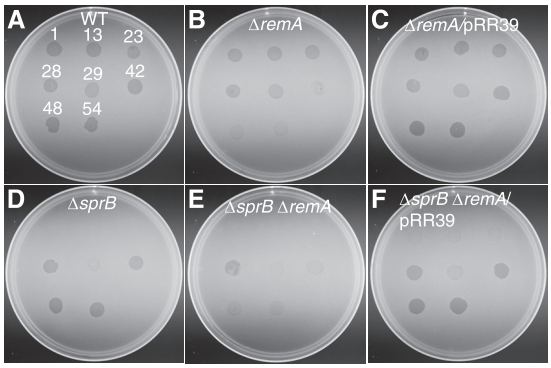

FIG 2 Effect of mutations on bacteriophage resistance. Bacteriophages (5 μl of lysates containing ~10^9 PFU/ml) were spotted onto lawns of cells in CYE overlay agar. The plates were incubated at 25°C for 24 h to observe lysis. Bacteriophages were spotted in the following order from left to right, as indicated also by the numbers in panel A: top row, ϕCj1, ϕCj13, and ϕCj23; middle row, ϕCj28, ϕCj29, and ϕCj42; bottom row, ϕCj48 and ϕCj54. (A) Wild-type *F. johnsoniae* CJ1827; (B) CJ1984 (Δ*remA*); (C) CJ1984 complemented with pRR39, which carries *remA*; (D) CJ1922 (Δ*sprB*); (E) CJ1985 (Δ*sprB* Δ*remA*); (F) CJ1985 complemented with pRR39.

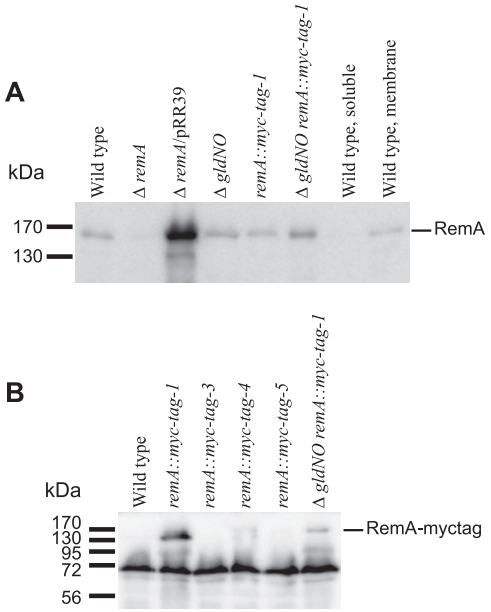

FIG 3 Immunodetection of RemA and RemA-myc-tag. (A) Cell extracts (15 μg of protein) were examined by Western blotting with antiserum against RemA. Lane 1, wild-type *F. johnsoniae* CJ1827; lane 2, CJ1984 (Δ*remA*); lane 3, CJ1984 complemented with pRR39 which carries *remA*; lane 4, CJ2090 [Δ(*gldN-gldO*)]; lane 5, CJ2083 (*remA*::myc-tag-1); lane 6, CJ2089 [Δ(*gldN-gldO*) *remA*::myc-tag-1]; lane 7, soluble (cytoplasmic and periplasmic) fraction of wild-type cell extract; lane 8, particulate (membrane) fraction of wild-type cell extract. (B) Cell extracts (20 μg of protein) were examined by Western blotting with antiserum against myc-tag peptide. Lane 1, wild-type *F. johnsoniae* CJ1827; lane 2, CJ2083 (*remA*::myc-tag-1); lane 3, CJ2077 (*remA*::myc-tag-3); lane 4, CJ2112 (*remA*::myc-tag-4); lane 5, CJ2073 (*remA*::myc-tag-5); lane 6, CJ2089 [Δ(*gldN-gldO*) *remA*::*myc-tag-1*].

(Δ*sprB* Δ*remA*) exhibited more dramatic motility defects, with most cells exhibiting little if any movement. The motility behavior of CJ1985 was similar to that of CJ1601 [Δ(*sprC sprD sprB*) *remA*::*HimarEm1*] (see Movie S1 in the supplemental material). Complementation of CJ1985 (Δ*sprB* Δ*remA*) with pRR39, which carries *remA*, restored motility comparable to or exceeding that exhibited by the parent strain CJ1922 (Δ*sprB*). The decreased motility of CJ1985 (Δ*sprB* Δ*remA*) compared to CJ1922 (Δ*sprB*) suggests that SprB and RemA may be partially redundant components of the motility apparatus. *sprB* mutants form nonspreading colonies as a result of motility defects, but colonies of the *remA* deletion mutant CJ1984 (Δ*remA*) were indistinguishable from those of the wild type (see Fig. S2 in the supplemental material), indicating that, unlike SprB, RemA is not required for movement of cells on agar.

RemA moves rapidly along the cell surface. RemA was predicted to be a cell-surface-exposed outer membrane protein. Antiserum against recombinant RemA was used to detect RemA in *F. johnsoniae* cell extracts. RemA was found in the insoluble fraction of cell extracts and migrated with an apparent molecular mass of ~150 kDa (Fig. 3A), which is close to the size predicted for the mature protein. Antiserum against RemA detected denatured protein in Western blots but failed to detect native RemA on the cell surface or in cell extracts. Four myc-tagged versions of *remA* were constructed and inserted into the genome in place of wild-type *remA*. Two of the strains, CJ2083 (*remA*::myc-tag-1; myc-tag inserted 150 bp downstream of the "A" in the start codon) and CJ2112 (*remA*::myc-tag-4; myc-tag inserted 2,286 bp downstream of the start codon), produced stable myc-tagged RemA protein, as detected by Western blotting (Fig. 3). These strains were sensitive to the same phages as were wild-type cells, suggesting that the myc-tagged versions of RemA localized properly and supported phage infection. Protein-G-coated latex spheres carrying antibodies against the myc-tag peptide bound specifically to cells of CJ2083 (*remA*::myc-tag-1) and CJ2112 (*remA*::myc-tag-4), indicating that RemA was exposed on the cell surface (Table 2). The bound spheres moved rapidly along the cell surface (see Movie S4 in the supplemental material), suggesting that RemA is propelled along the cell by the gliding "motor," as previously suggested for SprB (26). As previously reported (26, 31–34), and as shown in Table 2 and in Movie S4 in the supplemental material, Protein G-coated spheres did not bind to cells unless specific antiserum was added. They also failed to bind to wild type cells that did not express Myc-tagged RemA. Cells of CJ2077 (*remA*::myc-tag-3; myc-tag inserted 2,058 bp downstream of the start codon) and of CJ2073 (*remA*::myc-tag-5; myc-tag inserted 2,514 bp downstream of the start codon) produced little if any RemA and failed to bind protein-G-coated latex spheres carrying antibodies against the myc-tag peptide. To eliminate potential artifacts resulting from the relatively large (0.5-μm) latex spheres, the localization and movement of RemA-myc-tag-1 were also examined by immunofluorescence microscopy using antibodies against the myc-tag. Cells of CJ2083 expressed RemA-myc-tag-1 and were fluorescently labeled, whereas cells of CJ1827 (wild type) were not. The fluorescent antibodies moved smoothly along the cell surface at speeds of 1 to 2 μm/sec (Fig. 4; see Movie S5 in the supplemental material). The fluorescent signals traveled the length of the cell, looped around the pole, and returned to a location near the starting point, all within about 10 s. The movements of spheres and fluorescent antibodies are consistent with a model for gliding in which the gliding motor in the cell envelope propels cell-surface adhesins such as RemA. SprB, which also moves on the cell surface, was not required for RemA movement, since cells of CJ2072

TABLE 2 Binding of protein G-coated polystyrene spheres carrying antibodies against myc-tag peptide

Strain	Description	Antibody added	Avg (SD) % of cells with spheres attached[a]
CJ1827	Wild type	No antibody	0.6 (0.5)
CJ1827	Wild type	Anti-myc	0.6 (1.1)
CJ2083	*remA*::myc-tag-1	No antibody	0.0 (0.0)
CJ2083	*remA*::myc-tag-1	Anti-myc	52.3 (3.2)
CJ2077	*remA*::myc-tag-3	Anti-myc	0.0 (0.0)
CJ2112	*remA*::myc-tag-4	Anti-myc	33.3 (3.1)
CJ2073	*remA*::myc-tag-5	Anti-myc	0.3 (0.5)
CJ2089	Δ(*gldN-gldO*) *remA*::myc-tag-1	Anti-myc	0.0 (0.0)
CJ2089 with pTB79 carrying *gldN*	Δ(*gldN-gldO*) *remA*::myc-tag-1/pTB79 (*gldN*)	Anti-myc	52.0 (3.0)
CJ2097	*remA*::myc-tag-1 *sprF*	Anti-myc	52.6 (4.0)

[a] Purified anti-myc-tag antiserum and 0.5-μm-diameter protein G-coated polystyrene spheres were added to cells as described in Materials and Methods. Samples were introduced into a tunnel slide, incubated for 1 min at 25°C, and examined using a phase-contrast microscope. Images were recorded for 30 s, and 100 randomly selected cells were examined for the presence of spheres that remained attached to the cells during this time. The numbers in parentheses are standard deviations calculated from three measurements.

(Δ*sprB remA*::myc-tag-1) also propelled fluorescently labeled anti-myc antibodies (see Movie S5 in the supplemental material).

Mutations in *porSS* genes disrupt secretion of RemA. A novel protein secretion system, the Por secretion system (PorSS), is required for delivery of SprB to the cell surface, and also for secretion of an extracellular chitinase (33–35). A strain carrying myc-tagged *remA* and carrying a deletion of the region spanning the *porSS* genes *gldN* and *gldO* was constructed to determine whether the PorSS is involved in secretion of RemA. Cells lacking *gldN* and *gldO* produced myc-tagged RemA (Fig. 3) but failed to secrete it to the cell surface, as determined by the failure of latex spheres carrying antibodies against the myc-tag peptide to bind to the cells (Table 2). Complementation with pTB79, which carries *gldN*, restored surface exposure of myc-tagged RemA. The results suggest that the PorSS is required for secretion of RemA, in addition to its previously demonstrated roles in secretion of SprB and chitinase (33–35). SprB requires an additional protein, SprF, for secretion to the cell surface (31). SprF is thought to be an adapter to the PorSS that is specific for SprB, since SprF is not required for secretion of chitinase. Many of the *F. johnsoniae sprB* paralogs are adjacent to *sprF* paralogs, and the predicted SprF-like proteins may function in secretion of their cognate SprB-like proteins. *remA* does not have an *sprF*-like gene nearby. Cells of CJ2097 (*remA*::myc-tag-1 *sprF*) bound and propelled spheres carrying antibodies against the myc-tag peptide, indicating that SprF is not required for secretion of RemA (Table 2).

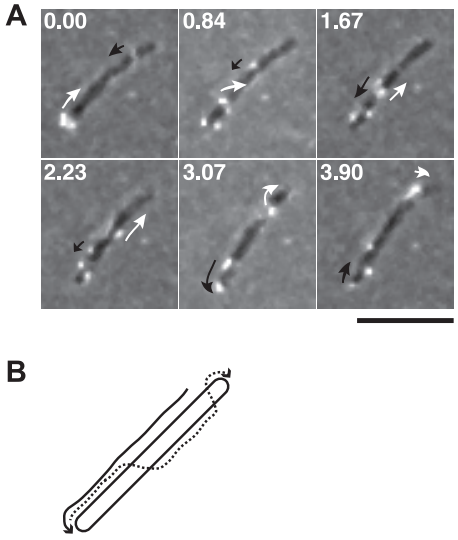

FIG 4 Movement of RemA on the cell surface. (A) Cells of CJ2083, which expressed RemA-myc-tag-1, were examined by a combination of immunofluorescence and phase-contrast microscopy. Low-light phase contrast was used to detect the cells, and antisera against the myc-tag peptide and goat anti-rabbit IgG conjugated to Alexa 488 were used to detect RemA-myc-tag-1. The sequence shown corresponds to the first 3.9 s of the third sequence (CJ2083 [RemA-myc-tag-1], with anti-myc-tag antibody) in Movie S5 in the supplemental material. The full movie includes controls demonstrating the specificity of the antiserum for the myc-tag peptide. Numbers in each panel indicate time in seconds. Arrows outline the apparent movements of two selected fluorescent signals. Bar, 5 μm. (B) Diagram illustrating the apparent movements of the two selected fluorescent signals highlighted in panel A over 3.9 s.

Analysis of the *remA* paralogs *fjoh_0803*, *fjoh_0804*, *fjoh_0805*, and *fjoh_0806*. Four *remA* paralogs lie near *remA* on the *F. johnsoniae* genome (Fig. 1). The products of *fjoh_0803*, *fjoh_0804*, *fjoh_0805*, and *fjoh_0806* exhibited 57, 47, 93, and 64% identities, respectively, to the C-terminal 500 amino acids of RemA and exhibited more limited similarity over the rest of RemA. The region of RemA between 725 and 830 amino acids, which corresponds to the lectin domain, was not conserved in the four *remA* paralogs. To determine whether the *remA* paralogs function in gliding and phage sensitivity, the region spanning *fjoh_0803-fjoh_0806* was deleted in wild-type cells, in CJ1984 (Δ*remA*) cells, and in CJ1985 (Δ*sprB* Δ*remA*) cells. Deletion of *fjoh_0803-fjoh_0806* from any of these strains had no effect on phage sensitivity, motility, or colony spreading (see Fig. S2 in the supplemental material and data not shown).

Involvement of RemA and cell-surface polysaccharides in cell-cell interactions. Wild-type *F. johnsoniae* cells grown in EC medium formed small cell aggregates (Fig. 5A). Cells of CJ1984 (Δ*remA*) were deficient in aggregate formation and complementation with *remA* on pRR39 restored the ability to form aggregates. The aggregates formed by the complemented strain were much larger than those formed by wild-type cells, suggesting that moderate overexpression of RemA from pRR39, which has a copy number of ~10, enhanced aggregation. Introduction of pRR39 into wild-type cells also enhanced aggregation. The control vector pCP23 did not cause cell aggregation, indicating that *remA* was responsible for this phenomenon. The large cell aggregates formed for strains carrying pRR39 resulted in rapid settling of the

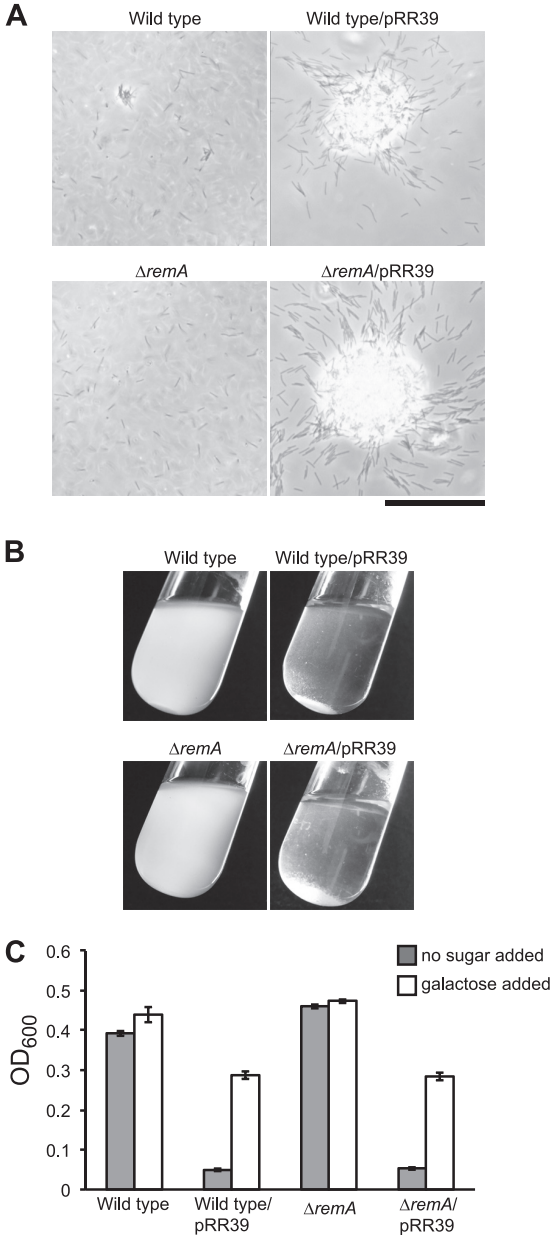

FIG 5 Effect of RemA on cell aggregation. Cells of CJ1827 (wild type) and CJ1984 (Δ*remA*) containing either control plasmid pCP23 (images on the left in panels A and B) or *remA*-expressing plasmid pRR39 (images on the right in panels A and B) were incubated in EC medium. (A) Observation of cells or cell clumps by phase-contrast microscopy. Bar, 50 μm. (B) Macroscopic observation of cell clumps in culture tubes. (C) Turbidity (OD_{600}) of samples taken from the top of the culture tubes. Measurements were obtained from samples taken directly from the tubes and from samples taken after addition of 5 mM D-galactose and incubation for 5 min to cause cell dispersal.

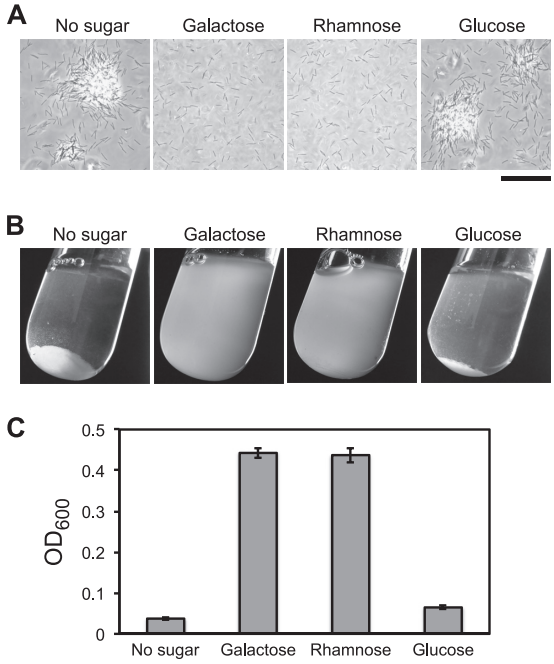

FIG 6 Effect of sugars on RemA-mediated cell aggregation. Cells of CJ1827 (wild type) carrying pRR39 to overexpress RemA were transferred into test tubes containing various sugars at final concentrations of 5 mM. Cultures were incubated with gentle shaking for 1 h at 23°C and examined for aggregation. (A) Observation of cells or cell clumps by phase-contrast microscopy. Bar, 50 μm. (B) Macroscopic observation of cell clumps in culture tubes. (C) Turbidity (OD_{600}) of samples taken from the top of the culture tubes.

cells from suspension, allowing macroscopic observation and quantitation of aggregation (Fig. 5B and C). The predicted lectin domain of RemA suggested the possibility that RemA bound to polysaccharides on the surface of neighboring cells. Addition of 5 mM D-galactose, L-rhamnose, or D-lactose resulted in the rapid dissolution of the aggregates, whereas the addition of other sugars (D-glucose, D-mannose, D-fructose, D-ribose, D-sorbitol, D-sucrose, D-maltose, and D-trehalose) at 5 to 100 mM did not (Fig. 6 and data not shown). The ability to completely disperse aggregates by adding 5 mM galactose allowed us to rapidly estimate total biomass by measuring the OD_{600} (Fig. 5C). Not surprisingly, the formation of large aggregates as a result of the overexpression of RemA correlated with decreased total biomass (Fig. 5C), probably because of reduced availability of nutrients or O_2 in the dense aggregates. As mentioned earlier, RemA moves rapidly on the cell surface (Fig. 4). The addition of galactose or rhamnose had no effect on the movement of RemA, as observed using antibody-coated spheres or by immunofluorescence microscopy (data not shown).

remC, *wza*, and *wzc* were identified in the same genetic screen that resulted in the identification of *remA*, and the proteins encoded by these genes are predicted to be involved in polysaccharide synthesis and secretion. Secreted polysaccharides might interact with RemA and be involved in cell-cell or cell-substratum interactions. pRR39 was introduced into cells of CJ1584 [Δ(*sprC sprD sprB*)], CJ1598 [Δ(*sprC sprD sprB*) *wza*::*HimarEm1*], CJ1602 [Δ(*sprC sprD sprB*) *wzc*::*HimarEm1*], and CJ1600 [Δ(*sprC sprD sprB*) *remC*::*HimarEm1*] in order to determine whether cells that overexpressed RemA but that were deficient in polysaccharide synthesis or secretion would form aggregates. Cell aggregates formed with CJ1584 carrying pRR39 but not with any of the strains with mutations in the predicted polysaccharide synthesis and secretion genes (Fig. 7). This suggests that both RemA and secreted polysaccharides are required for aggregate formation. RemA may function as a cell surface adhesin that interacts with polysaccharides synthesized and secreted by RemC, Wza, and Wzc. SprB, SprC, and SprD may also affect aggregate formation,

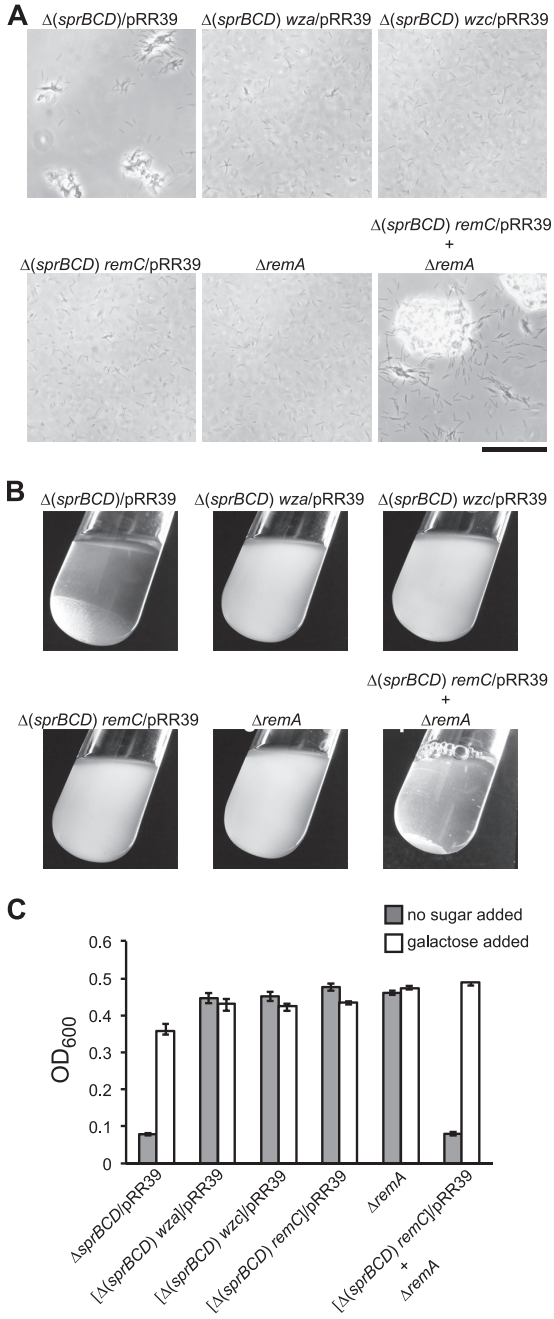

FIG 7 Effect of mutations in *remC*, *wza*, and *wzc* on cell aggregation. Cells of CJ1584 [Δ(*sprC sprD sprB*)], CJ1598 [Δ(*sprC sprD sprB*) *wza*::*HimarEm1*], CJ1602 [Δ(*sprC sprD sprB*) *wzc*::*HimarEm1*], CJ1600 [Δ(*sprC sprD sprB*) *remC*::*HimarEm1*], and CJ1984 (Δ*remA*) were incubated in EC medium. All strains carried pRR39 (to overexpress RemA) except for CJ1984 (Δ*remA*), which carried the control plasmid pCP23. To examine the ability of two nonaggregating strains to form aggregates when mixed together, 5 ml of CJ1600 [Δ(*sprC sprD sprB*) *remC*::*HimarEm1*] carrying pRR39 and 5 ml of CJ1984 (Δ*remA*) carrying pCP23 were mixed in a test tube and incubated for an additional 60 min. (A) Observation of cells or cell clumps by phase-contrast microscopy. Bar, 50 μm. (B) Macroscopic observation of cell clumps in culture tubes. (C) Turbidity (OD_{600}) of samples taken from the top of the culture tubes. Measurements were obtained from samples taken directly from the tubes and from samples taken after addition of 5 mM D-galactose, followed by incubation for 5 min to cause cell dispersal.

since the aggregates formed by cells of CJ1584 [Δ(*sprC sprD sprB*)] carrying pRR39 were smaller than those formed by wild-type cells carrying the same plasmid (Fig. 5A and 7A). However, although the overexpression of RemA (from pRR39) resulted in increased cell aggregation, the overexpression of SprB (from pSN60) did not (data not shown). Polysaccharide production and RemA expression do not need to occur in the same cell for aggregation to occur. Cells of CJ1984 (Δ*remA*), and of CJ1600 [Δ(*sprC sprD sprB*) *remC*::*HimarEm1*] carrying pRR39, neither of which formed aggregates in isolation, resulted in aggregate formation when they were mixed together (Fig. 7). Similar results were obtained when cells of CJ1984 were mixed with cells of the *wza* mutant CJ1598 carrying pRR39.

A fluorescent lectin was used to visualize secreted or cell surface polysaccharides or oligosaccharides on the cells of *F. johnsoniae*. Rhodamine-labeled *Ricinus communis* agglutinin I (RCA_{120}), which binds galactose, labeled cell clumps and individual cells. The fluorescent lectin was propelled rapidly on the cell surface (see Movie S6 in the supplemental material). This may indicate that some of the polysaccharide that was labeled with RCA_{120} also bound to RemA, so that the fluorescent lectin indirectly labeled RemA. Supporting this idea, strains lacking RemA failed to propel RCA_{120}. Cells of the *remC* mutant CJ1600 also failed to bind or propel RCA_{120}, suggesting that the putative glycosyltransferase RemC is involved in formation of the polysaccharide that is recognized by RCA_{120} (see Movie S7 in the supplemental material).

DISCUSSION

Gliding motility of *F. johnsoniae* is thought to involve motors composed of Gld proteins anchored in the cell envelope that propel the adhesin SprB along the cell surface (12, 26, 34). Mutants lacking SprB exhibit motility defects, but they are still able to move, albeit weakly, on glass. This suggested the possibility that additional mobile adhesins might function to allow movement over some surfaces and that SprB and these other adhesins may thus exhibit partial redundancy. Analysis of the *F. johnsoniae* genome revealed numerous potential *sprB* paralogs. A genetic approach was used to identify one *sprB* paralog, *remA*, which appears to encode a mobile cell surface adhesin that is partially redundant with SprB. Cells with mutations in *remA* exhibited motility defects that were only apparent when *sprB* was also defective. RemA and SprB are required for efficient infection by different *F. johnsoniae* bacteriophages and may function as receptors for these phages. Both SprB and RemA appear to rely on the PorSS for secretion to the cell surface. Additional SprB paralogs may also function in gliding and rely on the PorSS for secretion. This could explain why cells with mutations in the *porSS* genes *gldK*, *gldL*, *gldM*, and *gldN* exhibit complete resistance to bacteriophages and complete loss of motility (2, 33).

Previous experiments suggested that SprB moves rapidly along the cell surface (26). Analysis of myc-tagged versions of RemA revealed that RemA behaves similarly. Spheres coated with antibodies against the myc-tag peptide bound specifically to cells expressing RemA-myc-tag-1, and the spheres were rapidly propelled along the length of the cell, around the pole, and back down the other side. Cells expressing myc-tagged RemA also propelled fluorescently labeled anti-myc antibodies. Spheres and fluorescent labeled antibodies moved at speeds of approximately 1 to 2 μm per s, which is similar to the speed at which cells glide on glass. Anti-

bodies do not form permanent connections to their antigens, and it is possible for antibodies to tumble from one molecule of RemA to another. However, we do not expect the random tumbling of antibodies to be continuous and directional. The movements observed in the present study were rapid, continuous, and directional and indicate that RemA moves on the cell surface. The similar behaviors of SprB and RemA suggest that these cell surface proteins both interact with the motility apparatus. The apparent partial redundancy between these proteins may explain why cells lacking SprB retain some motility and why cells lacking SprB and RemA have a greater motility defect.

The apparent rapid continuous movements of SprB and RemA over long distances is unprecedented for bacterial proteins. SprB and RemA appear to move from pole to pole (5 to 10 μm) in a few seconds, whereas other outer membrane or cell surface proteins that have been studied, such as *E. coli* LamB, traveled <0.3 μm from their starting point during 5 min (6). Some cytoplasmic proteins such as MinC and peripheral cytoplasmic membrane proteins such as MinD do migrate rapidly in *E. coli* cells (10, 29, 30). These proteins cycle from pole to pole and back again (a distance of ~6 μm) in 40 to 50 s, but even these dramatic movements are considerably slower than those observed for the *Flavobacterium* motility adhesins.

RemA has a region that is similar in sequence to galactose/rhamnose-binding domains of SUEL-like lectins (37). Overexpression of RemA resulted in the formation of large aggregates of cells, and addition of galactose or rhamnose dispersed these aggregates. Cells of *remC*, *wza*, and *wzc* mutants, which are predicted to be defective for polysaccharide synthesis or secretion, failed to form large cell aggregates when RemA was overexpressed. Rhodamine-labeled lectin RCA_{120} interacted with wild-type cells and with cells that overexpressed RemA. RCA_{120} was rapidly propelled on the cell surface, which was reminiscent of the movements observed for RemA. RCA_{120} failed to interact with cells lacking the polysaccharide synthesis and secretion proteins RemC, Wza, and Wzc, and RCA_{120} was not propelled on the surface of cells lacking RemA. The simplest explanation for these results is that the extracellular polysaccharides interact with both RemA and with RCA_{120}. Interaction of RemA with polysaccharides could facilitate gliding of one cell over another cell or could facilitate movement of cells over other polysaccharide-coated surfaces. By producing and secreting polysaccharides that interact with RemA or other cell surface motility proteins, cells may essentially produce their own "road" and allow productive contact with a surface (such as perhaps glass) over which they might otherwise have difficulty moving. Cells could reuse such "roads" resulting in the multicellular patterns that are characteristic of *F. johnsoniae* swarms and colonies. A similar strategy for interacting with surfaces, involving secreted polysaccharides and polysaccharide-binding proteins, is used by the distantly related gliding bacterium, *Myxococcus xanthus*. Cells of *M. xanthus* move 50 times slower than those of *F. johnsoniae*, and they lack homologs for the *F. johnsoniae* motility proteins. *M. xanthus* uses two independent motility machineries: type IV pili for "S-motility" (40) and a separate motor system for "A-motility" (25, 36, 41). Secreted polysaccharides have been proposed to function in both motility systems (18, 43). The type IV pili interact with secreted polysaccharides containing glucosamine or *N*-acetylglucosamine (9, 16). Contact with a surface coated with polysaccharide results in pilus retraction and movement of the *M. xanthus* cell. Polysaccharides may also facilitate contact between proteins of the A-motility system and the substratum.

Our results support a model of *F. johnsoniae* motility in which gliding motors comprised of Gld proteins anchored in the cell envelope propel cell surface adhesins such as SprB and RemA (see Fig. S3 in the supplemental material). A similar model was proposed for the closely related bacterium "*Cytophaga*" sp. strain U67 in 1982, long before any of the components of the motility machinery had been identified (14). Some of the adhesins may interact directly with a surface, whereas others, such as RemA, may interact via secreted polysaccharides. The polysaccharides may coat the surface, forming a "road" over which cells travel. The action of the gliding "motors" on the adhesins attached to the substratum result in cell movement. *F. johnsoniae* cells glide on agar, glass, Teflon, polystyrene, and presumably many other surfaces in nature. Genome analyses suggest that *F. johnsoniae* has the ability to make many different adhesins and polysaccharides (24), which may explain the ability of cells to crawl over these diverse surfaces.

SprB and RemA are mobile cell surface adhesins involved in *F. johnsoniae* gliding, but many mysteries remain regarding the motors that propel these adhesins, and the sensory transduction (chemotaxis) system that allows cells to control their movements. Most of the Gld and Spr proteins lack sequence similarity to proteins of known function, and typical components of bacterial chemotaxis systems are absent in *F. johnsoniae*, so it is likely that novel aspects of *Flavobacterium* motility await discovery. SprB and RemA provide convenient handles to examine the functioning of the gliding machinery in living cells.

ACKNOWLEDGMENT

This research was supported by grant MCB-1021721 from the National Science Foundation.

REFERENCES

1. **Agarwal S, Hunnicutt DW, McBride MJ.** 1997. Cloning and characterization of the *Flavobacterium johnsoniae* (*Cytophaga johnsonae*) gliding motility gene, *gldA*. Proc. Natl. Acad. Sci. U. S. A. **94**:12139–12144.
2. **Braun TF, Khubbar MK, Saffarini DA, McBride MJ.** 2005. *Flavobacterium johnsoniae* gliding motility genes identified by *mariner* mutagenesis. J. Bacteriol. **187**:6943–6952.
3. **Braun TF, McBride MJ.** 2005. *Flavobacterium johnsoniae* GldJ is a lipoprotein that is required for gliding motility. J. Bacteriol. **187**:2628–2637.
4. **Chang LYE, Pate JL, Betzig RJ.** 1984. Isolation and characterization of nonspreading mutants of the gliding bacterium *Cytophaga johnsonae*. J. Bacteriol. **159**:26–35.
5. **Figurski DH, Helinski DR.** 1979. Replication of an origin-containing derivative of plasmid RK2 dependent on a plasmid function provided in trans. Proc. Natl. Acad. Sci. U. S. A. **76**:1648–1652.
6. **Gibbs KA, et al.** 2004. Complex spatial distribution and dynamics of an abundant *Escherichia coli* outer membrane protein, LamB. Mol. Microbiol. **53**:1771–1783.
7. **Godchaux W, III, Gorski L, Leadbetter ER.** 1990. Outer membrane polysaccharide deficiency in two nongliding mutants of *Cytophaga johnsonae*. J. Bacteriol. **172**:1250–1255.
8. **Godchaux W, Lynes IIIMA, Leadbetter ER.** 1991. Defects in gliding motility in mutants of *Cytophaga johnsonae* lacking a high-molecular-weight cell surface polysaccharide. J. Bacteriol. **173**:7607–7614.
9. **Hu W, et al.** 2012. Direct visualization of the interaction between pilin and exopolysaccharides of *Myxococcus xanthus* with eGFP-fused PilA protein. FEMS Microbiol. Lett. **326**:23–30.
10. **Hu Z, Lutkenhaus J.** 1999. Topological regulation of cell division in *Escherichia coli* involves rapid pole to pole oscillation of the division inhibitor MinC under the control of MinD and MinE. Mol. Microbiol. **34**:82–90.

11. **Hunnicutt DW, McBride MJ.** 2000. Cloning and characterization of the *Flavobacterium johnsoniae* gliding motility genes, *gldB* and *gldC*. J. Bacteriol. **182**:911–918.
12. **Jarrell KF, McBride MJ.** 2008. The surprisingly diverse ways that prokaryotes move. Nat. Rev. Microbiol. **6**:466–476.
13. **Kempf MJ, McBride MJ.** 2000. Transposon insertions in the *Flavobacterium johnsoniae ftsX* gene disrupt gliding motility and cell division. J. Bacteriol. **182**:1671–1679.
14. **Lapidus IR, Berg HC.** 1982. Gliding motility of *Cytophaga* sp. strain U67. J. Bacteriol. **151**:384–398.
15. **Li L-Y, Shoemaker NB, Salyers AA.** 1995. Location and characterization of the transfer region of a *Bacteroides* conjugative transposon and regulation of the transfer genes. J. Bacteriol. **177**:4992–4999.
16. **Li Y, et al.** 2003. Extracellular polysaccharides mediate pilus retraction during social motility of *Myxococcus xanthus*. Proc. Natl. Acad. Sci. U. S. A. **100**:5443–5448.
17. **Liu J, McBride MJ, Subramaniam S.** 2007. Cell-surface filaments of the gliding bacterium *Flavobacterium johnsoniae* revealed by cryo-electron tomography. J. Bacteriol. **189**:7503–7506.
18. **Lu A, et al.** 2005. Exopolysaccharide biosynthesis genes required for social motility in *Myxococcus xanthus*. Mol. Microbiol. **55**:206–220.
19. **McBride MJ.** 2001. Bacterial gliding motility: multiple mechanisms for cell movement over surfaces. Annu. Rev. Microbiol. **55**:49–75.
20. **McBride MJ.** 2004. *Cytophaga-Flavobacterium* gliding motility. J. Mol. Microbiol. Biotechnol. **7**:63–71.
21. **McBride MJ, Baker SA.** 1996. Development of techniques to genetically manipulate members of the genera *Cytophaga*, *Flavobacterium*, *Flexibacter*, and *Sporocytophaga*. Appl. Environ. Microbiol. **62**:3017–3022.
22. **McBride MJ, Braun TF.** 2004. GldI is a lipoprotein that is required for *Flavobacterium johnsoniae* gliding motility and chitin utilization. J. Bacteriol. **186**:2295–2302.
23. **McBride MJ, Kempf MJ.** 1996. Development of techniques for the genetic manipulation of the gliding bacterium *Cytophaga johnsonae*. J. Bacteriol. **178**:583–590.
24. **McBride MJ, et al.** 2009. Novel features of the polysaccharide-digesting gliding bacterium *Flavobacterium johnsoniae* as revealed by genome sequence analysis. Appl. Environ. Microbiol. **75**:6864–6875.
25. **Nan B, et al.** 2011. Myxobacteria gliding motility requires cytoskeleton rotation powered by proton motive force. Proc. Natl. Acad. Sci. U. S. A. **108**:2498–2503.
26. **Nelson SS, Bollampalli S, McBride MJ.** 2008. SprB is a cell surface component of the *Flavobacterium johnsoniae* gliding motility machinery. J. Bacteriol. **190**:2851–2857.
27. **Nelson SS, Glocka PP, Agarwal S, Grimm DP, McBride MJ.** 2007. *Flavobacterium johnsoniae* SprA is a cell-surface protein involved in gliding motility. J. Bacteriol. **189**:7145–7150.
28. **Pate JL, Petzold SJ, Chang L-YE.** 1979. Phages for the gliding bacterium *Cytophaga johnsonae* that infect only motile cells. Curr. Microbiol. **2**:257–262.
29. **Raskin DM, de Boer PA.** 1999. MinDE-dependent pole-to-pole oscillation of division inhibitor MinC in *Escherichia coli*. J. Bacteriol. **181**:6419–6424.
30. **Raskin DM, de Boer PA.** 1999. Rapid pole-to-pole oscillation of a protein required for directing division to the middle of *Escherichia coli*. Proc. Natl. Acad. Sci. U. S. A. **96**:4971–4976.
31. **Rhodes RG, Nelson SS, Pochiraju S, McBride MJ.** 2011. *Flavobacterium johnsoniae sprB* is part of an operon spanning the additional gliding motility genes *sprC*, *sprD*, and *sprF*. J. Bacteriol. **193**:599–610.
32. **Rhodes RG, Pucker HG, McBride MJ.** 2011. Development and use of a gene deletion strategy for *Flavobacterium johnsoniae* to identify the redundant motility genes *remF*, *remG*, *remH*, and *remI*. J. Bacteriol. **193**:2418–2428.
33. **Rhodes RG, et al.** 2010. *Flavobacterium johnsoniae gldN* and *gldO* are partially redundant genes required for gliding motility and surface localization of SprB. J. Bacteriol. **192**:1201–1211.
34. **Rhodes RG, Samarasam MN, Van Groll EJ, McBride MJ.** 2011. Mutations in *Flavobacterium johnsoniae sprE* result in defects in gliding motility and protein secretion. J. Bacteriol. **193**:5322–5327.
35. **Sato K, et al.** 2010. A protein secretion system linked to bacteroidete gliding motility and pathogenesis. Proc. Natl. Acad. Sci. U. S. A. **107**:276–281.
36. **Sun M, Wartel M, Cascales E, Shaevitz JW, Mignot T.** 2011. Motor-driven intracellular transport powers bacterial gliding motility. Proc. Natl. Acad. Sci. U. S. A. **108**:7559–7564.
37. **Tateno H.** 2010. SUEL-related lectins, a lectin family widely distributed throughout organisms. Biosci. Biotechnol. Biochem. **74**:1141–1144.
38. **Uenoyama A, Kusumoto A, Miyata M.** 2004. Identification of a 349-kilodalton protein (Gli349) responsible for cytadherence and glass binding during gliding of *Mycoplasma mobile*. J. Bacteriol. **186**:1537–1545.
39. **Vieria J, Messing J.** 1982. The pUC plasmids, an M13mp7-derived system for insertion mutagenesis and sequencing with synthetic universal primers. Gene **19**:259–268.
40. **Wall D, Kaiser D.** 1999. Type IV pili and cell motility. Mol. Microbiol. **32**:1–10.
41. **Wolgemuth C, Hoiczyk E, Kaiser D, Oster G.** 2002. How myxobacteria glide. Curr. Biol. **12**:369–377.
42. **Wolkin RH, Pate JL.** 1985. Selection for nonadherent or nonhydrophobic mutants co-selects for nonspreading mutants of *Cytophaga johnsonae* and other gliding bacteria. J. Gen. Microbiol. **131**:737–750.
43. **Yu R, Kaiser D.** 2007. Gliding motility and polarized slime secretion. Mol. Microbiol. **63**:454–467.